

PREPRINT:	Date: 1/4/1999	Rev: 1.0	Status: Physica B (in press)
-----------	----------------	----------	------------------------------

The asymmetric single-impurity Anderson model – the modified perturbation theory

D. Meyer, T. Wegner, M. Potthoff and W. Nolting

Institut für Physik, Humboldt-Universität zu Berlin, Invalidenstr. 110, 10115 Berlin, Germany

Abstract

We investigate the single-impurity Anderson model by means of the recently introduced *modified perturbation theory*. This approximation scheme yields reasonable results away from the symmetric case. The agreement with exactly known results for the symmetric case is checked, and results for the non-symmetric case are presented. With decreasing conduction band occupation, the breakdown of the screening of the local moment is observed. In the crossover regime between Kondo limit and mixed-valence regime, an enhanced zero-temperature susceptibility is found.

PACS

71.10.-w, 71.23.An, 75.20.Hr

Keywords

Single-impurity Anderson model, Modified perturbation theory, Dynamical mean-field theory (DMFT)

1 Introduction

The single-impurity Anderson model (SIAM) was originally introduced to describe magnetic impurities in weakly correlated non-magnetic metals [1]. It was successfully applied to explain unexpected low-temperature thermodynamic properties and photoemission data [2, 3]. Although its predictions for photoemission in periodic structures is still a matter of controversial discussions [4, 5, 6], it remains nevertheless surprisingly well suited for describing alloys of magnetic and non-magnetic compounds.

The SIAM is one of the most-examined and best-understood models of many-body physics. The renormalization group theory [7] and the Bethe-Ansatz (see e.g. [8]) have contributed enormously to the understanding of its physics. An excellent review of these and other theoretical approaches to the SIAM can be found in [9].

In the recent past, the SIAM has gained much interest in the context of the dynamical mean-field theory (DMFT) [10, 11]. It has been shown that in the limit of infinite dimensions, correlated lattice models can be mapped onto single-impurity models like the SIAM. Since the Bethe ansatz method requires special assumptions concerning the conduction band, it

is not applicable in the DMFT. Often, numerically exact methods such as *exact diagonalization* (ED) or *quantum Monte Carlo* (QMC) are used. Besides of being numerically expensive, there are also physical limitations to these methods. ED is principally limited to finite sized systems, while using QMC it is difficult to obtain results for low temperatures. Both methods are not well suited for calculating spectral densities. In addition to these methods, numerical renormalization group calculations to both the SIAM and via DMFT to the Hubbard model have been presented [12]. This method gives by construction very useful information for the low-energy behaviour, but the quality concerning high-energy features remains an open question. So there is still a need for reliable analytical methods.

A standard approximation scheme is second-order perturbation theory around the Hartree-Fock solution (SOPT-HF) [13]. In the context of the DMFT it is called *iterative perturbation theory* (IPT) [11]. This method gives convincing results at special parameter sets for the lattice problem, which map onto a particle-hole symmetric SIAM, but does not work very well for arbitrary system parameters. To extend the IPT to arbitrary band-fillings, an ansatz based on the SOPT-HF self-energy was introduced [14, 15, 16],

which reproduces the atomic limit and the Friedel sum rule [17, 18, 19] as well. On the basis of this ansatz, a further improvement was recently presented [20, 21] using the first four moments of the spectral density to determine the free parameters. The method (*modified perturbation theory* MPT) works away from the symmetric point and the magnetic properties of the solution [22] agree well with QMC results [23]. Since these results were obtained for the Hubbard model within the DMFT, it is still of interest to solve the original SIAM within the MPT. After outlining the main ideas of the MPT in the next section, we will discuss the results for the SIAM both in the symmetric and non-symmetric case. Comparison with exactly known results will provide a good basis to estimate the quality of the MPT.

2 Theory

The Hamiltonian of the SIAM reads as

$$H = \sum_{k,\sigma} (\epsilon_k - \mu) c_{k\sigma}^\dagger c_{k\sigma} + \sum_{k,\sigma} V_{kd} (c_{d\sigma}^\dagger c_{k\sigma} + c_{k\sigma}^\dagger c_{d\sigma}) + \sum_{\sigma} (\epsilon_d - \mu) n_{d\sigma} + \frac{U}{2} \sum_{\sigma} n_{d\sigma} n_{d-\sigma} \quad (1)$$

where $c_{k\sigma}^{(\dagger)}$ annihilates (creates) a conduction band electron with quantum numbers k and spin σ , ϵ_k is the corresponding eigenvalue of the conduction band Hamiltonian and μ the chemical potential. $c_{d\sigma}^{(\dagger)}$ annihilates (creates) an electron at the impurity-level ϵ_d . $n_{d\sigma} = c_{d\sigma}^\dagger c_{d\sigma}$ is the impurity occupation number operator. The hybridization strength between conduction band and impurity electrons is given by V_{kd} and enters all practical calculations via the hybridization function

$$\Delta(E) = \sum_k \frac{V_{kd}^2}{E + \mu - \epsilon_k} = V^2 \int dx \frac{\rho_0(x)}{E + \mu - x} \quad (2)$$

In this paper we assume the hybridization strength to be constant ($V_{kd} = V$), although this is not required for the MPT. $\rho_0(E)$ is the free density of states of the conduction electrons with bandwidth W . The impurity electrons interact with each other, where the interaction strength is U . Contrary to lattice models, e. g. the Hubbard model and the periodic Anderson model, the interaction takes place only at one single impurity level.

All relevant information can be obtained from the impurity Green function $G_{d\sigma}(E) = \langle \langle c_{d\sigma}; c_{d\sigma}^\dagger \rangle \rangle_E$ for

which we find the formal solution using the equation of motion

$$G_{d\sigma}(E) = \frac{1}{E + \mu - \epsilon_d - \Delta(E) - \Sigma_{d\sigma}(E)} \quad (3)$$

where we introduced the impurity self-energy $\Sigma_{d\sigma}(E)$. The actual problem is to find an (approximate) solution for the self-energy. We choose the modified perturbation theory [20], which was applied to the Hubbard model [21, 22] within the framework of the dynamical mean-field theory [10, 11]. Starting point is the following ansatz for the self-energy [16]:

$$\Sigma_{d\sigma}(E) = U \langle n_{d-\sigma} \rangle + \frac{a_\sigma \Sigma_{d\sigma}^{(\text{SOC})}(E)}{1 - b_\sigma \Sigma_{d\sigma}^{(\text{SOC})}(E)} \quad (4)$$

where $\Sigma_{d\sigma}^{(\text{SOC})}(E)$ denotes the second-order contribution to the SOPT-HF. The parameters a_σ and b_σ are chosen such that the first four spectral moments (up to $n = 3$)

$$M_{d\sigma}^{(n)} = \int dE E^n A_{d\sigma}(E) \quad (5)$$

are correctly reproduced.

$A_{d\sigma}(E) = (-1/\pi) \Im G_{d\sigma}(E + i0^+)$ is the spectral density. This requires [20]:

$$a_\sigma = \frac{\langle n_{d-\sigma} \rangle (1 - \langle n_{d-\sigma} \rangle)}{\langle n_{d-\sigma} \rangle^{(\text{HF})} (1 - \langle n_{d-\sigma} \rangle^{(\text{HF})})} \quad (6)$$

$$b_\sigma = \frac{B_{d-\sigma} - B_{d-\sigma}^{(\text{HF})} - (\mu - \tilde{\mu}_\sigma) + U(1 - 2\langle n_{d-\sigma} \rangle)}{U^2 \langle n_{d-\sigma} \rangle^{(\text{HF})} (1 - \langle n_{d-\sigma} \rangle^{(\text{HF})})} \quad (7)$$

where the superscript (HF) denotes Hartree-Fock expectation values. $B_{d\sigma}$ is a higher correlation function introduced by the fourth moment, which can be expressed in terms of dynamic one-particle quantities [20]

$$\begin{aligned} \langle n_{d\sigma} \rangle (1 - \langle n_{d\sigma} \rangle) (B_{d\sigma} - \epsilon_d) &= \\ &= \sum_k V_{kd} \langle c_{k\sigma}^\dagger c_{d\sigma} (2n_{d-\sigma} - 1) \rangle \\ &= -\frac{1}{\pi} \Im \int dE f_-(E) \Delta(E) \left(\frac{2}{U} \Sigma_{d\sigma}(E) - 1 \right) G_{d\sigma}(E) \end{aligned} \quad (8)$$

with the Fermi function $f_-(E) = (\exp(\beta E) + 1)^{-1}$. The results from reference [16] are simply recovered by replacing $B_{d\sigma}$ by its HF value:

$$\begin{aligned} \langle n_{d\sigma} \rangle^{(\text{HF})} (1 - \langle n_{d\sigma} \rangle^{(\text{HF})}) (B_{d\sigma}^{(\text{HF})} - \epsilon_d) &= \\ &= \sum_k V_{kd} \langle c_{k\sigma}^\dagger c_{d\sigma} \rangle^{(\text{HF})} (2\langle n_{d-\sigma} \rangle^{(\text{HF})} - 1) \\ &= -\frac{1}{\pi} \Im \int dE f_-(E) \Delta(E) \left(2\langle n_{d-\sigma} \rangle^{(\text{HF})} - 1 \right) G_{d\sigma}^{(\text{HF})}(E) \end{aligned} \quad (9)$$

The fictitious chemical potential $\tilde{\mu}_\sigma$ that appears in equation (7) is introduced as an additional parameter in the HF Green function

$$G_{d\sigma}^{(\text{HF})}(E) = \frac{1}{E + \tilde{\mu}_\sigma - \epsilon_d - \Delta(E) - U\langle n_{d-\sigma} \rangle} \quad (10)$$

It can be used to enforce for instance the Friedel sum rule as was done in [16], but one would restrict oneself to $T = 0$. Therefore, we choose the condition $\langle n_{d\sigma} \rangle = \langle n_{d\sigma} \rangle^{(\text{HF})}$ to fix $\tilde{\mu}_\sigma$ [20]. Thus, (6) is always simplified to $a_\sigma = 1$.

The modified perturbation theory constructed in that way reproduces several non-trivial limiting cases [20] such as $U/W^{(\text{eff})} \rightarrow 0$ ($W^{(\text{eff})} = V^2/W$ is the effective bandwidth of the impurity-level due to the hybridization) and $W^{(\text{eff})}/U \rightarrow 0$ (in the sense of [24]).

In the symmetric case (i. e. symmetric density of states, half filled conduction band and impurity level, $\epsilon_d = -U/2$) b_σ vanishes, and the ansatz (4) reduces to the SOPT-HF, since the latter reproduces the first four moments accidentally. It is known, that the SOPT-HF in the symmetric case gives reasonable results even for large U [25].

3 Results and discussion

3.1 The symmetric case

First we like to summarize the results for the symmetric case. In this case, the chemical potential will always be fixed at the center of gravity of the conduction band. In our calculations, the conduction band density of states is semi-elliptic and of unit width centered at $E = 0$, thus defining the energy scale used throughout this paper. In figure 1 (upper picture), the impurity quasiparticle density of states (QDOS) is plotted for various values of the hybridization strength V with constant $U = 1$. For all values of V , it consists of three structures. Two are located approximately at $-\frac{U}{2}$ and $\frac{U}{2}$, respectively. These correspond to the atomic quasiparticle levels ($\epsilon_d, \epsilon_d + U$) and are commonly called charge excitations. The central peak positioned at μ is usually denoted Kondo resonance (KR) [9]. This peak is a genuine many-body effect. The states responsible for this feature in the QDOS are ascribed to antiferromagnetic correlations between conduction electrons and the localized electrons on the impurity site which form a local moment. The antiferromagnetic correlations provide a screening of the local moment (Kondo screening) [9]. Both the width δ_K and height of the KR scale with V . The inset in figure 1 shows the variation of δ_K with V .

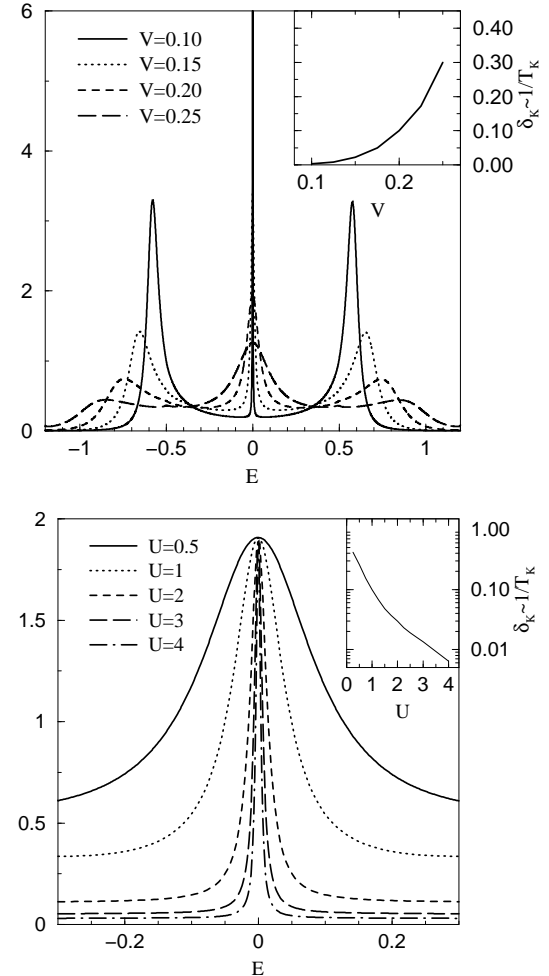


Figure 1: Impurity quasiparticle densities of state (impurity QDOS) of the symmetric SIAM ($\epsilon_d = -\frac{U}{2}$, $n_d = 1.0, n_c = 1.0, T = 0$). Top: $U = 1.0$ and different hybridization strengths V ; Bottom: $V = 0.2$ and various U . Only the vicinity of $E = \mu = 0$ is plotted. Inset: width δ_K of the Kondo resonance.

The Kondo resonance is plotted in the lower part of figure 1 for different values of U and constant V . The height is constant, since for the symmetric case, the MPT fulfills the Friedel sum rule as will be discussed below. The width δ_K varies as $\sim \frac{1}{1-\text{const}U^2}$.

The impurity susceptibility $\chi^{(\text{imp})}(T)$ is defined as the change of the susceptibility at the impurity site (denoted by i) due to the presence of the impurity:

$$\chi^{(\text{imp})}(T) = \frac{\partial \langle (n_{d\uparrow} + n_{ci\uparrow}) - (n_{d\downarrow} + n_{ci\downarrow}) \rangle}{\partial B} \Big|_{B \rightarrow 0} - \chi_i^{(0)}(T) \quad (11)$$

with $\chi_i^{(0)}$ being the susceptibility per lattice site of

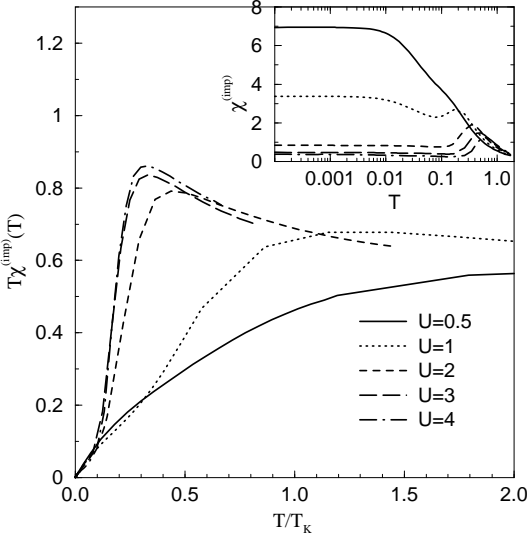


Figure 2: $T\chi^{(imp)}(T)$ and $\chi^{(imp)}(T)$ (inset) as functions of the temperature for the symmetric SIAM for different values of U ($V = 0.2$). The x-axis of the $T\chi^{(imp)}(T)$ -plot is normalized to the respective Kondo temperature (see text).

the pure system, i.e. without the impurity, and $n_{ci\sigma} = c_{i\sigma}^\dagger c_{i\sigma}$. Figure 2 shows $T\chi^{(imp)}(T)$ as a function of T . The temperature scale is normalized to the Kondo temperature defined by $T_K = \frac{1}{\chi^{(imp)}(T=0)}$ [26]. This quantity is proportional to the inverse width of the KR: $T_K \sim \frac{1}{\delta_K}$ [9]. For large values of U , a scaling behaviour is observable, the susceptibility as function of $\frac{T}{T_K}$ is approximately independent of U . For high temperatures, $\chi^{(imp)}(T)$ becomes Curie-like: $\chi^{(imp)}(T) \sim \frac{1}{T}$. Thus the impurity behaves like a local moment of size $T\chi^{(imp)}(T)$. For low temperatures, strong deviations from the Curie law are obvious. For small U , $\chi^{(imp)}(T)$ becomes flat, showing Pauli-like behaviour. For $U \gtrsim 2.0$ (Kondo limit), the susceptibility develops a maximum, the position of which scales with T_K and marks the onset of the screening of the local moment. For $T \rightarrow 0$, the susceptibility is Pauli-like again, but with reduced value.

In summary, for the symmetric SIAM the MPT calculations, which are equivalent to SOPT-HF in this case, agree well with expected or exactly known results [9]. This is of course due to the fact, that for the symmetric SIAM, the perturbation series for the self-energy converges rapidly even for large U [25].

3.2 The asymmetric case

In this section, we present results for the non-symmetric SIAM. Away from the symmetric point, less results are known exactly. Furthermore, standard perturbation theory cannot give as convincing results as in the symmetric case.

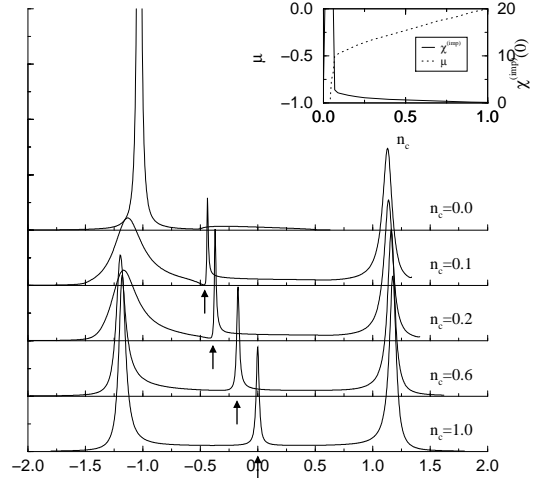


Figure 3: Impurity QDOS of the non-symmetric SIAM: $U = 2$, $\epsilon_d = -1.$, $V = 0.2$, $T = 0$, but various n_c . The chemical potential is positioned at the arrows. The inset shows the chemical potential μ and the susceptibility $\chi^{(imp)}(T = 0)$ as function of the conduction band occupation n_c .

First we study the variation of the conduction band occupation number n_c . Starting from the symmetric case with $U = 2$ and $V = 0.2$, we vary n_c between 1 and 0. Correspondingly, the chemical potential shifts towards lower energies. In figure 3, the QDOS for different n_c is plotted. The arrows indicate the position of the chemical potential μ . The inset shows $\chi^{(imp)}(T = 0)$ and μ as function of n_c . With decreasing n_c , the Kondo resonance also shifts to lower energies. Note that for $n_c < 1$ the chemical potential lies below the center of the KR, which additionally becomes rather asymmetric. For very low carrier concentration n_c , the KR disappears. For most carrier concentrations is the zero-temperature susceptibility almost constant, only a slight increase with reducing n_c is visible. At $n_c \approx 0.07$, however, $\chi^{(imp)}(0)$ diverges. This divergence is directly related to the disappearance of the Kondo resonance. Exactly at $n_c = 0.07$, the chemical potential μ crosses the lower edge of the conduction band. There are no electrons which could form (via antiferromagnetic correlations) a Kondo resonance, thus no screening occurs. The still occupied impurity states of the lower charge ex-

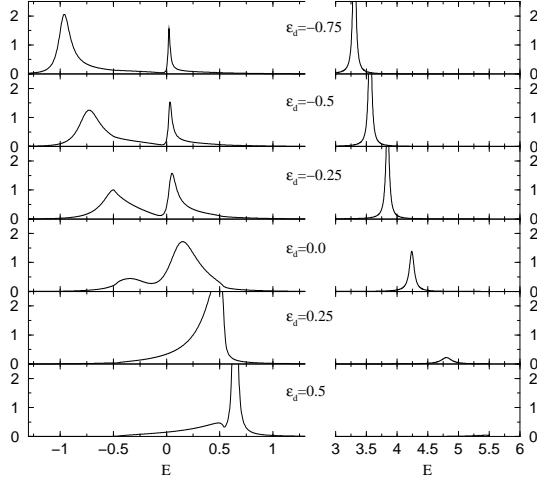


Figure 4: Impurity QDOS for different values of ϵ_d and constant $U = 4$, $V = 0.2$, $n_c = 1.0$ (therefore $\mu = 0$).

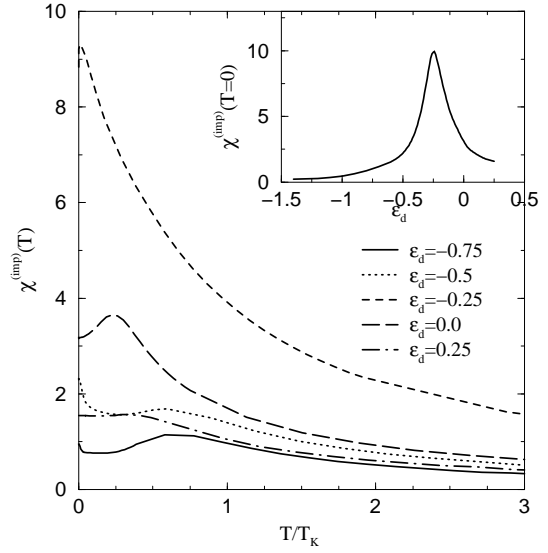


Figure 5: $\chi^{(imp)}(T)$ for the parameter sets of figure 4.

citation peak form a local moment. Since now $\chi^{(imp)}$ is the susceptibility of a stable local moment, the divergence is to be expected. Only for $n_c = 0$ the susceptibility vanishes completely. This is, because the chemical potential shifts to $\mu \rightarrow -\infty$, and the impurity level is therefore also empty.

Next, we like to investigate another asymmetric situation: we fix U to a large constant value of $U = 4$ and vary the energetic position of the impurity ϵ_d with respect to the conduction band. The hybridization strength is set to $V = 0.2$ and the occupation number of the conduction band $n_c = 1$. The latter implies $\mu = 0$. The situation is visualized by means of the impurity QDOS in figure 4. The lower charge excitation peak moves with increasing ϵ_d from below ($\epsilon_d = -0.75$) into the conduction band. The upper charge excitation at approximately $\epsilon_d + U$ also moves towards higher energies. Contrary to the charge excitation peaks, the Kondo resonance remains at its position $E = \mu = 0$. For $\epsilon_d \gtrsim 0$ the KR merges into the lower charge excitation peak. The upper charge excitation loses spectral weight as the impurity level becomes depopulated. For $\epsilon_d \gtrsim 0.5$, a dip indicates the onset of a gap within the lower charge excitation. This gap will simply separate the charge excitation from hybridization-induced states within the conduction band and is not a correlation effect.

In particular, figure 4 shows that within the MPT the charge excitation peaks are positioned close to the atomic quasiparticle levels as expected. Contrary, within the SOPT-HF the positions do not significantly depend on ϵ_d .

The transition from the Kondo limit to the intermediate valence regime (IV) and finally to the empty-impurity state manifests itself in the susceptibility (see figure 5). For high temperatures the susceptibility follows Curie's law, $\chi^{(imp)}(T) \sim \frac{1}{T}$ in all three cases. Only for low temperatures, $\chi^{(imp)}(T)$ behaves differently for the respective parameter regimes. In the Kondo limit ($\epsilon_d \lesssim -0.5$, solid and dashed line)), $\chi^{(imp)}(T)$ shows a maximum and decreases for decreasing temperature. For very low $T \lesssim 0.1T_K$ an increase is visible, for even lower temperatures, the susceptibility becomes constant again and $\frac{\partial}{\partial T}\chi^{(imp)}(T)|_{T=0} = 0$ (not recognizable in figure 5). In the IV-regime, and most pronounced around $\epsilon_d \approx -0.25$, the $\frac{1}{T}$ -behaviour persists down to much lower temperatures, the zero-temperature susceptibility is enlarged, and therefore the Kondo temperature T_K becomes smaller. This can be ascribed to a weaker screening of the local moment. A further increase of ϵ_d depopulates the impurity. The “effective local moment” shrinks and the susceptibility gets reduced. The T -axis in figure 5 is normalized to T_K using the definition mentioned in section 3.1. No scaling behaviour is visible.

The above-mentioned enhancement of $\chi^{(imp)}(T)$ in the Kondo regime for low temperatures, which is most clearly observable for $\epsilon_d = -0.5$ needs further discussion. This feature is obviously most pronounced at the crossover from the Kondo limit to the IV-regime. An interesting observation can be made by examining the impurity density of states $\rho_d(E)$ at $E = \mu = 0$.

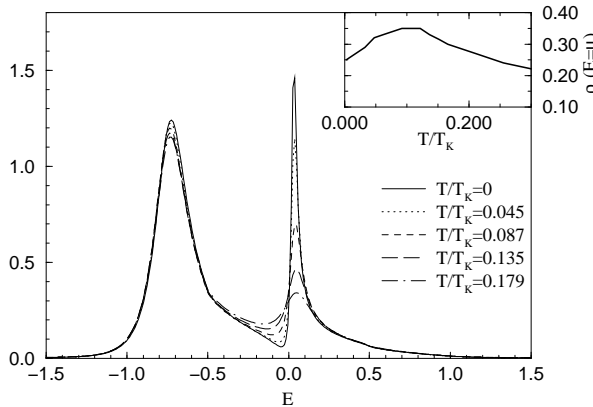


Figure 6: Lower part of the impurity QDOS for $\epsilon_d = -0.5$, $U = 4$, $V = 0.2$ and $n_c = 1.0$ at various temperatures. The inset shows the value of the impurity QDOS $\rho_d(E)$ at $E = \mu = 0$.

For $\epsilon_d = -0.5$ (see figure 6), it shows a maximum at the same temperature where the increase of the susceptibility begins. For ϵ_d away from -0.5 , this maximum becomes less pronounced and eventually disappears. With its disappearance the characteristic increase of the susceptibility also vanishes. This as well as the concurrence of the position of the maximum and the onset of the increase of the susceptibility suggest a closer relation of the behaviour of $\rho_d(\mu)$ and $\chi^{(imp)}(T)$. However, it is astounding that a decrease of $\rho_d(\mu)$ provokes an increase in $\chi^{(imp)}(T)$. One possibility to explain this behaviour is the following: The states, that build up the Kondo resonance, are responsible for the screening of the local moment. In the examined non-symmetric case, most spectral weight of the KR lies above μ (see figure (6)). Only those electrons filling the states close to the chemical potential contribute to the screening. If $\rho_d(\mu)$ goes down, the number of electrons participating in the screening decreases. The screening should become less effective. Eventually, the local moment, which is still present, shows a stronger reaction to an applied magnetic field. Consequently, the susceptibility increases. In this way, the observation may be understood.

To finish our survey of the asymmetric SIAM, we like to check the Friedel sum rule [9, 17] numerically. The Friedel sum rule relates the occupation number of the impurity level, $\langle n_{d\sigma} \rangle$, to the real part of the

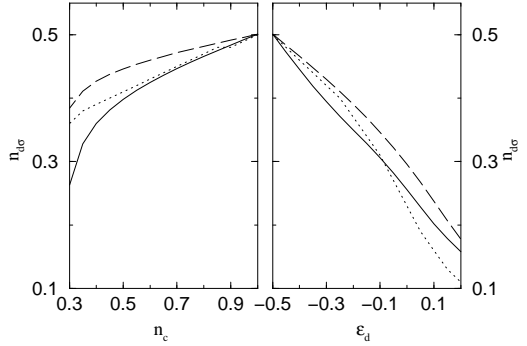


Figure 7: Test of the Friedel sum rule for the asymmetric SIAM. The impurity occupation is plotted as dotted line, the result for the impurity occupation using the Friedel sum rule as solid line (dashed line: SOPT-HF result). Left picture: $U = 1.0$, $V = 0.2$, $\epsilon_d = -0.5$; right picture: $U = 1.0$, $V = 0.2$, $n_c = 1.0$.

self-energy at the Fermi energy:

$$\langle n_{d\sigma} \rangle = \frac{1}{2} - \frac{1}{\pi} \arctan \left(\frac{\epsilon_d + \Re \Sigma_\sigma(0) + \Re \Delta(0)}{\Im \Delta(0)} \right) \quad (12)$$

This formula can be derived using the Luttinger theorem [18] as shown in [9, 19].

For the symmetric SIAM, (12) becomes trivially fulfilled in the MPT (equivalently in the second order perturbation theory) since $\Re \Delta(0) = 0$, $\Re \Sigma_\sigma(0) = \frac{U}{2}$ and $\epsilon_d = -\frac{U}{2}$. Therefore the impurity occupation is always $\langle n_{d\sigma} \rangle = 0.5$. Our results for the asymmetric case are plotted in figure 7. The dotted line is the impurity occupation $\langle n_{d\sigma} \rangle$ within our approximation. The solid line (dashed line) is obtained using (12) with the MPT (SOPT-HF) self-energy. In the left picture, the conduction band occupation n_c is varied from 0.3 to 1. The other parameters are chosen such that the right boundary represents the symmetric case for $U = 1$. As discussed above, in the symmetric point both the MPT and the SOPT-HF fulfill the Friedel sum rule. For $n_c \lesssim 1$, however, the SOPT-HF deviates almost immediately, whereas in the MPT, the Friedel sum rule is met in excellent agreement until $n_c \approx 0.55$. For lower n_c , the deviation increases. The origin of this breakdown within our theory is not yet clarified. The right picture shows the situation of fixed values of $U = 1$ and $n_c = 1$, ϵ_d being varied. For the left boundary, the parameters are identical to the right boundary of the left picture (symmetric point). Varying ϵ_d away from the symmetric point both the MPT and the SOPT-HF do not fulfill the Friedel sum rule. However, in this case, the superiority of the MPT relative to the SOPT-HF still

manifests itself in the correct positions of the charge excitations (figure 4). The SOPT-HF fails to reproduce these.

4 Conclusions

We have analysed the SIAM within the modified perturbation theory (MPT). For the symmetric SIAM, the MPT and therefore our results are equivalent to the SOPT-HF. In this case, the SOPT-HF gives reasonable results even for large values of U [25]. For the asymmetric case, the SOPT-HF does not work very well. This may be due to the fact that the SOPT-HF fails to reproduce the first four moments of the spectral density. However, the MPT, which by construction always fulfills these moments, gives reasonable results also away from the symmetric point. Within the MPT, the positions and weights of the charge excitations are predicted correctly since this is closely related to the first four moments [22]. Furthermore, we achieve a better agreement with the Friedel sum rule compared to the SOPT-HF.

Concluding, one can state that the MPT yields reasonable results in a wide region of the parameter space. Its conceptual simplicity and its numerical feasibility qualify the MPT as a valuable complement to the QMC method in the context of DMFT.

Acknowledgement

Financial support of the *Deutsche Forschungsgemeinschaft* within the project **No 158/5-1** as well as the support of the *Friedrich-Naumann Stiftung* for one of us (D. M.) is gratefully acknowledged.

References

- [1] P. W. Anderson, Phys. Rev. **124**(1), 41 1961.
- [2] O. Gunnarson and K. Schönhammer, Phys. Rev. B **31**, 4815 1985.
- [3] J. W. Allen, S. J. Oh, O. Gunnarson, K. Schönhammer, M. B. Maple, M. S. Torikachvili, and I. Lindau, Adv. in Phys. **35**, 275 1986.
- [4] A. J. Arko, J. J. Joyce, A. B. Andrews, J. D. Thompson, J. L. Smith, E. Moshopoulo, Z. Fisk, A. A. Menovsky, P. C. Canfield, and C. G. Olson, Physica B **230-232**, 16 1997.
- [5] S. Hüfner, Ann. Phys. **5**, 453 1996.
- [6] D. Malterre, M. Grioni, and Y. Baer, Adv. Phys. **45**(4), 299 1996.
- [7] K. Wilson, Rev. Mod. Phys. **47**(4), 773 1975.
- [8] A. M. Tsvelick and P. B. Wiegmann, Advances in Physics **32**(4), 453 1983.
- [9] A. C. Hewson, *The Kondo Problem to Heavy Fermions*, Cambridge University Press 1993.
- [10] W. Metzner and D. Vollhardt, Phys. Rev. Lett. **62**, 324 1989.
- [11] A. Georges, G. Kotliar, W. Krauth, and M. J. Rozenberg, Rev. Mod. Phys. **68**(1), 13 1996.
- [12] R. Bulla, A. C. Hewson, and T. Pruschke, J. Phys.: Condens. Matter **10**, 8365 1998.
- [13] G. Bulk and R. J. Jelitto, Phys. Rev. B **41**, 413 1990.
- [14] A. Martin-Rodero, F. Flores, M. Baldo, and R. Pucci, Solid State Commun. **44**, 911 1982.
- [15] A. Martin-Rodero, E. Louis, F. Flores, and C. Tejedor, Phys. Rev. B **33**, 1814 1986.
- [16] H. Kajueter and G. Kotliar, Phys. Rev. Lett. **77**(1), 131 1996.
- [17] J. Friedel, Can. J. Phys. **34**, 1190 1956.
- [18] J. M. Luttinger and J. C. Ward, Phys. Rev. **118**(5), 1417 1960.
- [19] D. Langreth, Phys. Rev. **150**(2), 516 1966.
- [20] M. Potthoff, T. Wegner, and W. Nolting, Phys. Rev. B **55**(24), 16132 1997.
- [21] T. Wegner, M. Potthoff, and W. Nolting, Phys. Rev. B **57**(11), 1 1998.
- [22] M. Potthoff, T. Herrmann, T. Wegner, and W. Nolting, phys. stat. sol. (b) **210**, 199 1998.
- [23] M. Ulmke, Eur. Phys. J. B **1**, 301 1998.
- [24] A. Harris and R. Lange, Phys. Rev. **157**(2), 295 1967.
- [25] V. Zlatić and B. Horvatić, Phys. Rev. B **28**(12), 6904 1983.
- [26] M. Jarrell, Phys. Rev. B **51**(12), 7429 1995.